

Title	Dynamics of Dilute Polymer Solution in Couette Flow : Dynamic Light Scattering Experiments on Polystyrene-Latex Particles in Water (Commemoration Issue Dedicated to Professor Tetsuya HANAI On the Occasion of His Retirement)
Author(s)	Tsunashima, Yoshisuke; Odani, Hisashi
Citation	Bulletin of the Institute for Chemical Research, Kyoto University (1991), 69(4): 322-330
Issue Date	1991-12-30
URL	<a href="http://hdl.handle.net/2433/77411">http://hdl.handle.net/2433/77411</a>
Right	
Type	Departmental Bulletin Paper
Textversion	publisher

# Dynamics of Dilute Polymer Solution in Couette Flow. Dynamic Light Scattering Experiments on Polystyrene-Latex Particles in Water

Yoshisuke TSUNASHIMA\* and Hisashi ODANI\*

*Received August 7, 1991*

A method to examine polymer dynamics in solution under flow field is presented. Dynamic light scattering technique is applied to dilute aqueous suspensions of polystyrene-latex particles in simple shear flow. The observed flow-enhanced twisting correlation function can be explained in terms of the particle diffusion and the convection of the particle subjected to shear gradient.

**KEY WORDS:** Dynamic Light Scattering/Shear Flow/Polystyrene-latex Particles/Particle Diffusion/Particle Convection/

## INTRODUCTION

Recent dynamic light scattering (DLS) studies of dilute polymer solutions at equilibrium are providing new information about polymer chain dynamics. These studies reveal that the hydrodynamic description of dilute polymer solutions so far proposed is still insufficient to explaining the experimental results, as is typically demonstrated by works of the present author.<sup>1</sup> Nonequilibrium studies may thus throw new light on the hydrodynamic description of polymer chains. However, we have had few such studies except for recent theoretical ones on the hydrodynamic equation of polymer solutions under shear flow.<sup>2-4</sup> In this paper, we present the brief description of DLS measurements in flow and discuss the dynamical behavior of polystyrene-latex particles in dilute aqueous solutions subjected to steady simple shear flow of very small gradient.

## THEORETICAL

Consider a single-frequency laser light of the characteristic width  $w$  plunged into a dilute solution of small rigid particles and measure the scattered light from the solution through two fine pinholes which serve to collimate a part of the scattered beam, that is, the scattering volume. The heterodyne correlation function,  $F_1(\mathbf{q}, t)$ , for the scattered light has the form

$$F_1(\mathbf{q}, t) = \sum_{j=1}^N \langle E_j^*(0) E_j(t) \exp \{ i\mathbf{q} \cdot [\mathbf{r}_j(t) - \mathbf{r}_j(0)] \} \rangle \quad (1)$$

Here  $\mathbf{q}$  is the scattering vector defined by  $\mathbf{q} = \mathbf{k}_i - \mathbf{k}_s$  with  $\mathbf{k}_i$  and  $\mathbf{k}_s$  the incident- and

\* 網島 良祐, 小谷 壽: Laboratory of fundamental Material Properties, Institute for Chemical Research, Kyoto University Uji, Kyoto 611, Japan.

the scattered-light wave vector, respectively. For the vertically polarized light, it follows that  $|\mathbf{q}| = (4\pi n/\lambda_0)\sin(\theta/2)$ , where  $\theta$  is the scattering angle,  $n$  is the refractive index of the fluid, and  $\lambda_0$  is the wavelength of the incident light in vacuum.  $E_j(t)$  is the amplitude of the light scattered by particle  $j$  and  $\mathbf{r}_j(t)$  is the center-of-mass position of particle  $j$  at time  $t$ . The summation is over all particles in the scattering volume and the angle brackets denote an ensemble average over experimental realization.

If the particles are spherical and optically homogeneous and make Brownian motions in the quiescent fluid, eq 1 gives a single exponential decay characterizing the particle translational diffusion

$$F_1(\mathbf{q}, t) = \exp(-Dq^2 t) \quad (2)$$

where  $D$  represents the translational diffusion coefficient of the particle. In the presence of shear flow field  $V$ , however, eq 1 should be treated as described below.

We here introduce two time scales,  $\tau_t$  and  $\tau_s$ . The  $\tau_t$  represents the transit time of a particle across the scattering volume;  $\tau_t = w/|U|$  with  $U$  the mean particle velocity in the scattering volume. The amplitude function  $E_j(t)$  in eq 1 thus varies with the time scale of  $\tau_t$ . The  $\tau_s$ , on the other hand, is the time scale characteristic of the phase factor  $\exp(i\mathbf{q} \cdot [\mathbf{r}(t) - \mathbf{r}(0)])$  in eq 1 and represents the shortest time for which a particle in shear flow field  $V$  traverses over a length scale  $|\mathbf{q}|^{-1}$ ;  $\tau_s = (\mathbf{q} \cdot \mathbf{V}_{\max})^{-1} = (q_V \gamma w)^{-1}$  where  $\mathbf{V}_{\max}$  is the maximum shear velocity in the scattering volume and  $\gamma$  is the velocity gradient. For a limit  $\tau_t/\tau_s \ll 1$ , the amplitude factor is dominant in eq 1, that is, the number of particles in the scattering volume changes so quickly that measurement of  $F_1(\mathbf{q}, t)$  corresponds to the single beam velocimetry. For the opposite limit  $\tau_t/\tau_s \gg 1$ , the particle moves only a short distance relative to  $w$  on the time scale  $\tau_s$  and the amplitude factor in eq 1 is essentially constant over  $\tau_s$ . In this case and as is usual when the laser beam could be focused down to the order  $w \sim 10^{-2}$  cm, eq 1 can be simplified into a form

$$\begin{aligned} F_1(\mathbf{q}, t) &= \sum_{j=1}^N \langle E_j^*(0) E_j(t) \rangle \langle \exp\{i\mathbf{q} \cdot [\mathbf{r}_j(t) - \mathbf{r}_j(0)]\} \rangle \\ &= \sum_{j=1}^N I_j F_{sj}(\mathbf{q}, t) \end{aligned} \quad (3)$$

Here  $I_j$  is the scattered light intensity of particle  $j$ ;  $I_j = \langle E_j^*(0) E_j(0) \rangle$ . The so-called self-intermediate scattering function,  $F_{sj}(\mathbf{q}, t)$ , is related to the probability distribution  $G_{sj}(\mathbf{R}, t)$  for particle  $j$  to suffer a displacement  $\mathbf{R}$  in the time  $t$ ;  $G_{sj}(\mathbf{R}, t) = \langle \delta(\mathbf{R} - [\mathbf{r}_j(t) - \mathbf{r}_j(0)]) \rangle$ .

For systems where the particle  $j$  has a velocity  $V_j$ , the  $G_{sj}(\mathbf{R}, t)$  can be regarded as the solution to the classical convection-diffusion equation for the particle<sup>5</sup>

$$\partial [G_{sj}(\mathbf{R}, t)] / \partial t = D \nabla_{\mathbf{R}}^2 G_{sj}(\mathbf{R}, t) - \nabla_{\mathbf{R}} \cdot [V_j G_{sj}(\mathbf{R}, t)] \quad (4)$$

subject to the initial condition that  $G_{sj}(\mathbf{R}, 0) = \delta(\mathbf{R})$ . Furthermore, the velocity  $V_j$  can

be approximated as

$$V_j = \bar{V}_j + \mathbf{I} \cdot \mathbf{R}_j \quad (5)$$

in the present light scattering experiments where the convection or diffusion process is characterized by the maximum length scale of the scattering volume,  $w$ . In eq 5,  $\bar{V}_j$  is the mean velocity of particle  $j$  at the position  $\mathbf{R} = \mathbf{r}_j$  and  $\mathbf{I}$  is the local velocity gradient tensor. The spatial Fourier transform of eq 4 is then

$$\partial [F_{sj}(\mathbf{q}, t)] / \partial t = -Dq^2 F_{sj}(\mathbf{q}, t) + i\mathbf{q} \cdot \bar{\mathbf{V}}_j F_{sj}(\mathbf{q}, t) + \mathbf{q} \cdot \mathbf{I} \nabla_{\mathbf{q}} F_{sj}(\mathbf{q}, t) \quad (6)$$

Taking first the Laplace transform of eq 6, and then solving the resulting equation for  $\tilde{F}_{sj}(\mathbf{q}, s)$ , the Laplace transform of  $F_{sj}(\mathbf{q}, t)$ , and again Laplace inverting the function  $\tilde{F}_{sj}(\mathbf{q}, s)$ , we can solve eq 6. The solution subject to the boundary condition that  $F_{sj}(\mathbf{q}, 0) = 1$  is<sup>6</sup>

$$F_{sj}(\mathbf{q}, t) = \exp\left\{-\int_0^t [Dp^2(t) + i\bar{\mathbf{V}}_j \cdot \mathbf{p}(t)] dt\right\} \quad (7)$$

$$\mathbf{p}(t) = \mathbf{q} \exp(-\mathbf{I}^T t) \quad (8)$$

The heterodyne correlation function  $F_1(\mathbf{q}, t)$  can be obtained by substituting eqs 7 and 8 into eq 3. If the number of particles in the scattering volume is large, the sum in eq 3 can be transformed to a volume integral. Moreover, the mean velocity of particle  $j$ , i.e.,  $\bar{\mathbf{V}}_j$  in eq 7, can be replaced by the velocity averaged over all particles in the scattering volume,  $\mathbf{U}$ , the velocity  $\mathbf{U}$  being approximately related to the velocity of particles  $\mathbf{V}(\mathbf{R})$  at  $\mathbf{R}$  as

$$\mathbf{V}(\mathbf{R}) = \mathbf{U} + \mathbf{V} = \mathbf{U} + \mathbf{I} \cdot \mathbf{R} \quad (9)$$

Here the distinct expression of eq 9 from eq 5 should be noted. On the approximations mentioned above, the heterodyne correlation function  $F_1(\mathbf{q}, t)$  becomes

$$F_1(\mathbf{q}, t) = \exp\left\{-\int_0^t dt [Dp^2(t) + i\mathbf{U} \cdot \mathbf{p}(t)]\right\} \iiint d\mathbf{R} I(\mathbf{R}) \exp\left\{-i \int_0^t dt \mathbf{p}(t) \cdot \mathbf{I} \cdot \mathbf{R}\right\} \quad (10)$$

where  $I(\mathbf{R})$  is the intensity profile of the incident beam in the scattering volume. The corresponding homodyne correlation function  $F_2(\mathbf{q}, t)$  is

$$\begin{aligned} F_2(\mathbf{q}, t) &= 1 + |F_1(\mathbf{q}, t)|^2 = 1 + F_1(\mathbf{q}, t) F_1^*(\mathbf{q}, t) \\ &= 1 + \exp\left\{-2 \int_0^t dt Dp^2(t)\right\} \left| \iiint d\mathbf{R}^3 I(\mathbf{R}) \exp\left\{-i \int_0^t dt \mathbf{p}(t) \cdot \mathbf{I} \cdot \mathbf{R}\right\} \right|^2 \\ &\quad \mathbf{p}(t) = \mathbf{q} \exp(-\mathbf{I}^T t) \end{aligned} \quad (11)$$

The first equation holds for the case of flowing particles where the time scale of  $F_1(\mathbf{q},$

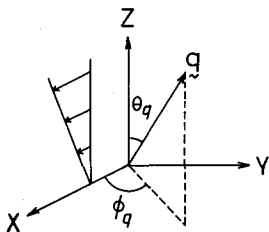


Fig. 1. The scattering geometry for the imposed shear flow.  $\mathbf{q}$  is the scattering vector. The flow is in the  $X$  direction.

$t$ ) is sufficiently short compared to the exchange time of scattering volumes under shear flow,  $\tau_f$ , which is defined by  $\tau_f = w / V_{\max} = w / \gamma w = \gamma^{-1}$ . It is interesting to note that  $F_2(\mathbf{q}, t)$  does not depend on the mean velocity  $U$ , while does the case for  $F_1(\mathbf{q}, t)$ .

For simple shear flow where

$$\mathbf{\Gamma} = \gamma \begin{pmatrix} 0 & 0 & 1 \\ 0 & 0 & 0 \\ 0 & 0 & 0 \end{pmatrix}$$

and the direction of flow is aligned along the  $X$  axis, as shown in Figure 1, the velocity gradient term in eq 11 becomes<sup>6</sup>

$$\begin{aligned} & \left| \iiint dR^3 I(R) \exp\left\{-i \int_0^t dt \mathbf{p}(t) \cdot \mathbf{\Gamma} \cdot \mathbf{R}\right\} \right|^2 = \left| \iiint dR^3 I(R) \exp(-iq_x \gamma z t) \right|^2 \\ & = \exp\left\{-(1/2)(q_x \gamma \omega t)^2\right\} \end{aligned} \quad (12)$$

The last equation can be obtained on the assumption that the intensity profile of the incident beam  $I(R)$  is Gaussian with mean square spread  $w^2$ . Eq. 11 then gives the final form<sup>6</sup>

$$\begin{aligned} A(t) & \equiv F_2(\mathbf{q}, t) \\ & = 1 + \exp\left\{-2Dq^2 t [1 + \gamma t \sin\theta_q \cos\theta_q \cos\phi_q \right. \\ & \quad \left. + (1/3)\gamma^2 t^2 \sin^2\theta_q \cos^2\theta_q] - (1/2)(q_x \gamma \omega t)^2\right\} \end{aligned} \quad (13)$$

This expression shows that the homodyne correlation function in shear flow,  $A(t)$ , varies on three independent time scales:

$$\tau_D \equiv (Dq^2)^{-1}, \quad \tau_f \equiv \gamma^{-1}, \quad \tau_s \equiv (q_x \gamma \omega)^{-1}$$

These time scales correspond to the particle translational diffusion, the translation across the scattering volume, and the particle convection due to the local velocity gradient, respectively. The shape of  $F_2(\mathbf{q}, t)$  thus depends strongly on an experimental set-up and the particle motions in a given solution. The ratio  $\tau_f/\tau_s$  will typically be  $O(10^3)$ , following which we can refer to the two cases: For particles of  $D \sim 10^{-7}$  cm<sup>2</sup>/s, the other ratios will be estimated as  $\tau_f/\tau_D \sim O(10^3)$  and  $\tau_D/\tau_s \sim O(1)$ , which situation

provides the basis for determining the two time scales,  $\tau_D$  and  $\tau_s$ , from homodyne experiments. For particles of  $D \sim 10^{-10}$  cm<sup>2</sup>/s, on the other hand, the time scale  $\tau_s$  will be dominant because  $\tau_D/\tau_s \sim O(10^3)$  and  $\tau_f/\tau_D \sim O(1)$ .

### EXPERIMENTAL AND DISCUSSION

Aqueous suspensions of polystyrene-latex particles of 0.091  $\mu\text{m}$  diameter (Dow chemical) was diluted with distilled water to concentration of  $3 \times 10^{-5}$  g/g solution. The solution was then filtered through a Millipore filter (0.22  $\mu\text{m}$  pore size) into a gap between inner (rotating) and outer (stationary) cylinders of a rotating cylinder viscometer. The inner and outer cylinders are of 0.6cm and of 0.8cm radius, respectively, and are made of glass. Steady simple shear flow of a very low shear stress of  $10^{-3}$  dynes/cm<sup>2</sup> was yielded in the gap of 0.2cm width by an eddy-current drive of the inner floating cylinder (rotor), the control of which drive was performed with a permanent magnet rotated by a geared synchronous motor.

As shown in Figure 2, a vertically polarized single-frequency argon-ion laser beam of 488nm line (Spectra-Physics, Model 2020-03/2560) was plunged normally to the concentric outer and inner cylinders and was focused on their axial center. Under a given shear flow, the intensity fluctuation of the light (vertical component) scattered from the solution at the middle point of the gap was measured through our laboratory-made software correlator of 512 channels. The scattering volume was hence character-

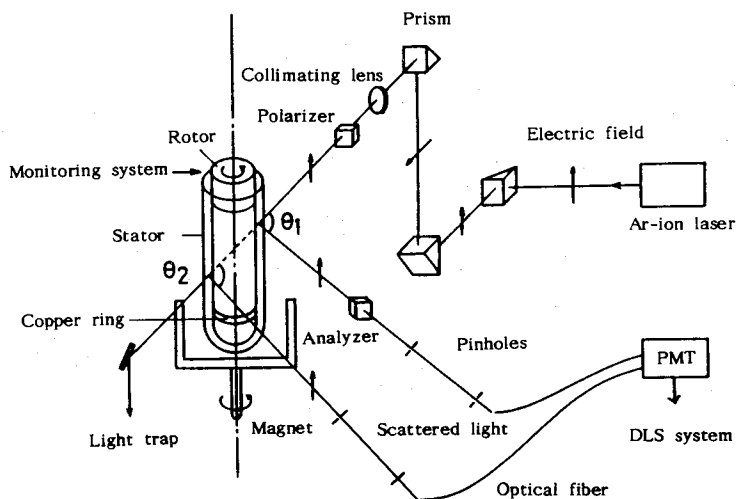


Fig. 2. The experimental set-up for the dynamic light scattering in shear flow. A single-frequency 488nm line emitted from an etalon-equipped argon-ion laser source is incident upon the gap between the rotor and the stator. The vertical or horizontal arrow indicated on the incident or the scattered beam shows the direction of the incident or the scattered electric field vector. The rotor is driven synchronously. The driving torque is produced through the interaction of the rotating magnetic field with the magnetic moment induced by the eddy-current in a copper ring which is set in the bottom of the rotor. An angle  $\theta_1$  or  $\theta_2$  represents a supplementary angle to the scattering angle  $\theta$ :  $\theta = \pi/2 - \theta_1$ .

ized by the laser-beam width  $w$  ( $\approx 0.017\text{cm}$ ) and by a pair of pinholes of  $0.03\text{cm}$  diameter, the pinholes being set  $30\text{cm}$  apart each other. The relative viscosity of the solution to the solvent water  $\eta_r$  was also measured simultaneously by counting the number of rotation of the rotor:

$$\eta_r \equiv \eta/\eta_0 = (\omega_{R,0}/\omega_R) [(\omega_M - \omega_R)/(\omega_M - \omega_{R,0})] \quad (14)$$

Here  $\eta$  and  $\eta_0$  are the viscosity of the solution and of the solvent, respectively.  $\omega_i$  is the angular velocity of the rotor (suffix  $i=R$ ) or the magnet (suffix  $M$ ), and the suffix 0 denotes its solvent value. The shear gradient  $\gamma$  at the middle point of the gap can also be estimated as

$$\gamma = 4\omega_R [R_1^2 R_2^2 / (R_2^2 - R_1^2)^2] \ln(R_2/R_1) \quad (15)$$

with  $R_1$  and  $R_2$  the radius of the rotor and of the stationary cylinder (stator), respectively.

Figure 3 shows the experimental coordinate system for the imposed shear flow and for the incident laser beam. The shear flow is in the  $X$  direction and its gradient appears in the  $Z$  direction, as described already:

$$V_x = \gamma Z, \quad V_y = V_z = 0 \quad (16)$$

The incident beam is in the  $Z$  direction (i.e.,  $k_i$  is normal to the flow direction) and the scattered light is measured in the plane of shear, i.e.,  $k_s$  is in the  $XZ$  plane. This means that the scattering vector  $q$  is in the plane of shear ( $\phi_q = 0$  in Fig.1) and its angle against the  $Z$  direction  $\theta_q$  is related to the scattering angle  $\theta$  as

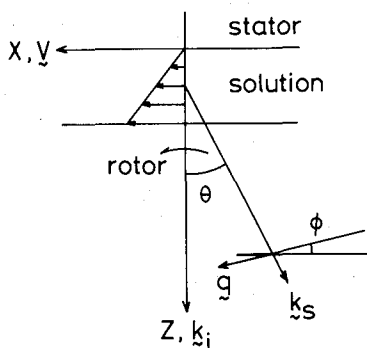


Fig. 3. The experimental coordinate system. The rotor (inner cylinder) is driven counterclockwise. The shear flow of gradient  $\gamma$  is produced in the  $X$  direction in the gap between the stator (outer cylinder) and the rotor. The scattered light from the solution at the middle point of the gap is measured at the scattering angle  $\theta$  with a photon-counting photomultiplier tube (PMT), which is connected to the software correlator.

$$\theta_q = \pi/2 - \theta/2 \quad (17)$$

At  $\theta_q = \pi/2$ ,  $\mathbf{q}$  is aligned along the direction of flow. Moreover, the  $X$  component of  $\mathbf{q}$  becomes to be  $q_x = q_v = q \cos \phi$  with  $\phi = \theta/2$ .

The dynamic light scattering measurements were made at 25.0°C for aqueous suspensions of polystyrene-latex particles. The mass concentration was  $3 \times 10^{-5}$  g/g solution. As an example, the  $A(t)$  behavior at different shear gradients is demonstrated in Figure 4. Here the scattering angle  $\theta$  is 85° and  $\gamma$  is set at 0 (quiescent solution), 0.367, 0.764, and 1.72 s<sup>-1</sup>. In the figure, the 511 data points are tried to be fitted to a single-exponential-type decay curve (a solid line), as is usual in the analysis of  $A(t)$  for quiescent polymer solutions. At  $\gamma \leq 0.764$  s<sup>-1</sup>, the data points locate completely on the solid curve, its decay rate, defined by  $\Omega \equiv Dq^2$ , being 2910 s<sup>-1</sup>. This value is coincident with the calculated one from the translational diffusion coefficient  $D_{\text{calc}}$  for the present polystyrene-latex particles of 0.091 μm size;  $\Omega_{\text{calc}} = D_{\text{calc}} q^2 = 2903$  s<sup>-1</sup>. The diffusion mode of the time scale  $\tau_D$ , which is to be  $\tau_D = 1/\Omega_{\text{calc}} = 3.44 \times 10^{-4}$  s, is thus overwhelmingly dominant at  $\gamma \leq 0.764$  s<sup>-1</sup>. However,  $A(t)$  data lose the single-exponential-decay nature at  $\gamma = 1.72$  s<sup>-1</sup>. It seems to twist around a data-fitted solid curve of the decay rate  $\Omega = 4060$  s<sup>-1</sup>. This means that, at  $\gamma = 1.72$  s<sup>-1</sup>, the second mode of time scale  $\tau_s$

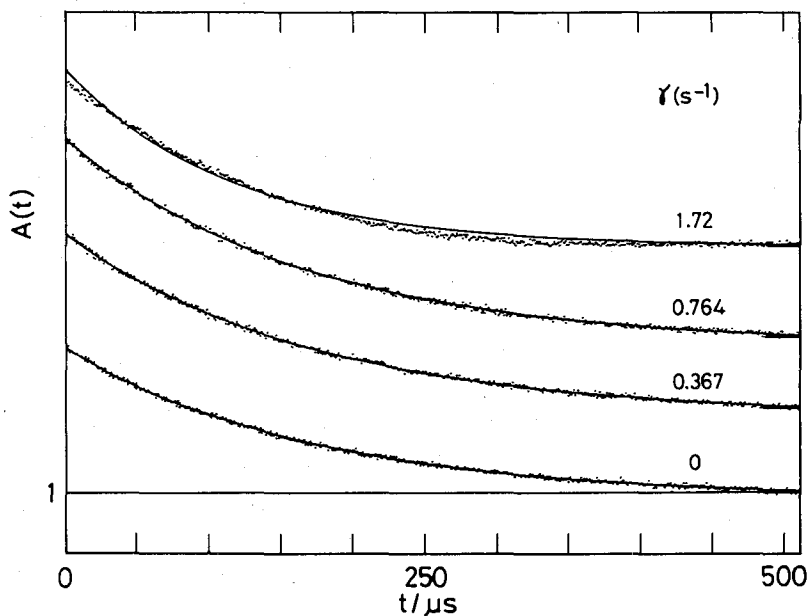


Fig. 4. The homodyne correlation function  $A(t)$  is plotted against time  $t$  for aqueous suspensions of polystyrene-latex particles at the scattering angle 85° and at 25°C. The magnitude of the shear gradient  $\gamma$  is changed as indicated in the figure. The base line of each  $A(t)$ , i.e., the ordinate at  $A(t)=1$ , is shifted upwards except for that at  $\gamma=0$ . Data-fitted solid curves are of single-exponential decay.



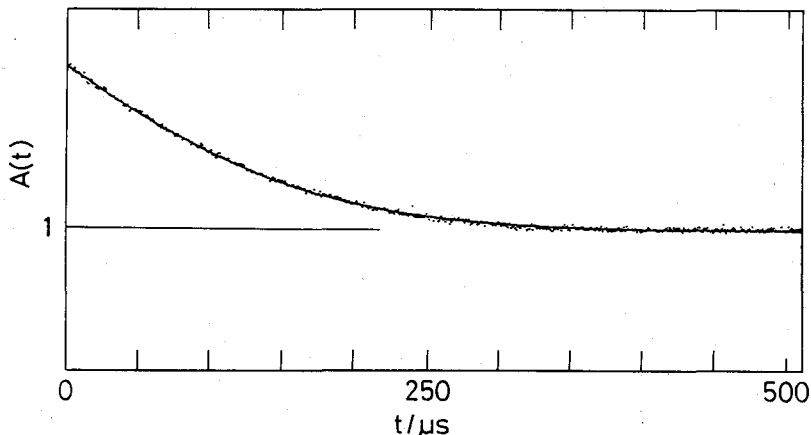


Fig. 5. The reanalysis of the  $A(t)$  data at  $\gamma=1.72 \text{ s}^{-1}$ . The solid curve represents the  $A(t)$  calculated from eq 13 with two time scales,  $\tau_D$  and  $\tau_s$ .

comes to effective in  $A(t)$  as well as the  $\tau_D$  mode.

In order to analyze the  $A(t)$  data at  $\gamma=1.72 \text{ s}^{-1}$ , we estimate the magnitude of  $\tau_s$  and  $\tau_f$  in eq 13. With  $\theta=85^\circ$  and  $w=0.0171 \text{ cm}$ , it follows that  $\tau_s=(q_x\gamma w)^{-1}=1.99\times 10^{-4} \text{ s}$ , which value is comparable to the previous  $\tau_D$  value, while  $\tau_f(=\gamma^{-1})$  is as large as 0.58 s. Since the contribution of  $\tau_f$  to  $A(t)$  in eq 13 is negligibly small, we can express the  $A(t)$  by a quadratic form of  $t$ ;  $B\exp[-(2/\tau_D)t-(1/2\tau_s^2)t^2]$  with  $B$  the amplitude factor. The solid curve in Figure 5 represents the  $A(t)$  thus estimated from the quadratic form, in the process of which analysis the  $\tau_D$  and  $\tau_s$  were fixed at the previously mentioned values and  $B$  was treated as a fitting parameter. Almost all data points are explained by the solid curve, as shown in the figure. This gives us a conclusion that  $A(t)$  at  $\gamma=1.72 \text{ s}^{-1}$  contains two time-scales,  $\tau_D$  and  $\tau_s$ , whose magnitudes are of nearly the same order;  $\tau_D=3.44\times 10^{-4} \text{ s}$  and  $\tau_s=1.99\times 10^{-4} \text{ s}$ . The deviation of the  $A(t)$  data at  $\gamma=1.72 \text{ s}^{-1}$  in Figure 4 from the single exponential decay is hence due to the  $\tau_s$  mode characterized by the inverse sigmoidal-type decay.

It is noticed in Figure 5 that the data points remain unfitted to the estimated solid curve at  $t>250 \mu\text{s}$ ; they show an oscillatory or a downward deviation, though it is not clear because its magnitude is very small. The deviation might be attributed to the fluctuation of  $\gamma$  with time or the shear-induced aggregation<sup>7-9</sup> of the latex particles in solution. However, the discussion is beyond the framework of the present paper. Experiments at larger  $\gamma$  will offer information on such a phenomenon, which discussion will be made in the forthcoming paper.<sup>10</sup>

#### ACKNOWLEDGMENTS

We acknowledge the financial support of the Grant-in-Aid for Scientific Research (B) 01470106.

REFERENCES

- (1) (a) Y. Tsunashima, M. Hirata, N. Nemoto, and M. Kurata, *Macromolecules* **20**, 1992(1987).  
(b) Y. Tsunashima, M. Hirata, N. Nemoto, K. Kajiwara, and M. Kurata, *Macromolecules* **20**, 2862(1987).  
(c) Y. Tsunashima, *Polymer* **30**, 2284(1989).
- (2) Y. Rabin, S. Q. Wang, and K. F. Freed, *Macromolecules* **22**, 2420(1989).
- (3) W. Zylka and H. C. Öttinger, *Macromolecules* **24**, 484(1991).
- (4) J. A. Y. Johnson, *Macromolecules* **20**, 103(1987).
- (5) B. J. Berne and R. Pecora, *Dynamic Light scattering*; Wiley, New York, 1976.
- (6) W. Stasiak and C. Cohen, *J. Chem. Phys.* **79**, 5718(1983).
- (7) (a) A. Onuki, *Phys. Rev. Lett.* **62**, 2472(1989).  
(b) A. Onuki *J. Phys. Soc. Jpn.* **59**, 3427(1990).
- (8) (a) M. Doi and D. Chen, *J. Chem. Phys.* **90**, 5271(1989).  
(b) D. Chen and M. Doi, *J. Chem. Phys.* **91**, 2656(1989).
- (9) E. Helfand and G. H. Fredrickson, *Phys. Rev. Lett.* **62**, 2468(1989).
- (10) Y. Tsunashima, in press.